HANSSON, R., HAYES, P.C., and JAK, E. Phase equilibria in the Fe-Zn-O system at conditions relevant to zinc sintering and smelting. *VII International Conference on Molten Slags Fluxes and Salts,* The South African Institute of Mining and Metallurgy, 2004.

# Phase equilibria in the Fe-Zn-O system at conditions relevant to zinc sintering and smelting

R. HANSSON, P.C. HAYES, and E. JAK
*PYROSEARCH, Pyrometallurgy Research Centre, The University of Queensland, Australia*

Zincite and spinel phases are present in the complex slag systems encountered in zinc/lead sintering and zinc smelting processes. These phases form extensive solid solutions and are stable over a wide range of compositions, temperatures and oxygen partial pressures. Accurate information on the stability of these phases is required in order to develop thermodynamic models of these slag systems.

Phase equilibria in the Fe-Zn-O system have been experimentally studied for a range of conditions, between 900 and 1580°C and oxygen partial pressures ($pO_2$) between air and metallic iron saturation, using equilibration and quenching techniques. The compositions of the phases were measured using Electron Probe X-ray Microanalysis (EPMA). The ferrous and ferric bulk iron concentrations were determined using a specially developed wet-chemical analysis procedure based on the use of ammonium metavanadate. XRD was used to confirm phase identification. A procedure was developed to overcome the problems associated with evaporation of zinc at low $pO_2$s and to ensure the achievement of equilibria. An isothermal section of the system $FeO$-$Fe_2O_3$-$ZnO$ at high ZnO concentrations at 1200°C was constructed. The maximum solubilities of iron and zinc in zincite and spinel phases in equilibrium were determined at $pO_2=1*10^{-6}$ atm at 1200 and 1300°C.

The morphology of the zincite crystals sharply changes in air between 1200 and 1300°C from rounded to plate-like. This is shown to be associated with significant increase in total iron concentration, the additional iron being principally in the form of ferric iron.

Calculations performed by FactSage with a thermodynamically optimized database have been compared with the experimental results.

Keywords: Phase Equilibria, Fe-Zn-O, Quenching, Wet-Chemistry, EPMA, XRD, ISP.

## Introduction

Industrial zinc and lead/zinc smelting slags are described by the seven component system $ZnO$-$PbO$-$Al_2O_3$-$CaO$-$FeO$-$Fe_2O_3$-$SiO_2$. The high melting temperature phases zincite $(Zn,Fe)O$ and spinel $(Zn,Fe)(Fe,Zn)_2O_4$ are commonly formed in these slags at typical operating conditions influencing the liquidus temperatures and physico-chemical properties of the slag. The morphology of zincite has also been found to play a key role in the performance of sinters in the Imperial Smelting Process (ISP).

The ISP is used to process complex zinc/lead sulphide concentrates and secondary zinc-containing materials. Most of the sulphur is removed in an oxidizing sinter roast. Fine-grained primary and secondary feeds are sintered into agglomerates during the roasting. The sintered material is subsequently fed to the upper part of the Imperial Smelting Furnace (ISF) As the charge descends the shaft, reduction of zinc and lead oxides takes place. The physical and chemical properties of the sinter have been shown to influence the ISF performance. Holliday *et al.*[1–2] investigated effects of premature softening of sinter in the upper shaft of the ISF. They concluded that high softening temperatures are beneficial and that softening temperatures are determined by the formation of the zincite refractory network that, in turn, requires zincite having a plate-like shape. Lee and Hayes[3] observed both rounded and plate-like zincite containing low and high concentrations of iron respectively during their study on reduction of ISP sinters. Zhao *et al.*[4] found that if ISP sinters contain round-shaped zincite and a high proportion of connected glass the softening temperature is low; and if sinters contain a plate-like-shaped zincite and, therefore, a continuous network of refractory crystals, then sinter softens at much higher temperatures. In both the sintering process under oxidizing conditions, and during descent through the ISF shaft under reducing conditions, the sinter materials contain significant fractions of liquid phase. The volume fractions and compositions of the liquids present influence the efficiencies of the sintering and reduction processes, and the control of slag fluid characteristics. Phase equilibrium information is therefore crucial for the understanding and control of the microstructure of the ISP sinter and its transformation and behaviour in the ISF.

Knowledge of the phase relations and compositions in lower order (binary and ternary) systems are also crucial for the development and optimization of thermodynamic models of higher order slag systems. The $FeO$-$Fe_2O_3$-$ZnO$ ternary system is part of the seven component $ZnO$-$PbO$-$Al_2O_3$-$CaO$-$FeO$-$Fe_2O_3$-$SiO_2$ system. Phase equilibria in this ternary system explain the relations and stabilities of zinc ferrite, wustite and zincite solid solutions around the ZnO-rich corner crucial for the performance of the ISP. Very little information has previously been reported on ferric and ferrous iron concentrations in the phases close to the ZnO-rich corner. More experimental studies especially at intermediate $pO_2$s are needed on this system. A simultaneous optimization of the complete seven-component system, including data on liquid slag in equilibrium with solid spinel and zincite cannot be performed satisfactory without experimentally confirmed relations and extent of solid solutions of phases formed in the lower order systems.

## Experimental

### Equilibration and quenching in air followed by EPMA

The experimental procedure used in the present study is similar to that described by Jak *et al.*[5]. Powders of the $Fe_2O_3$ and ZnO 99.5+ wt pct purity and Fe powder 99.9+ wt pct purity were used as starting materials. Pure powders of the oxides were weighed and then mixed thoroughly in an agate mortar. The mixtures were pelletized, and equilibrated in platinum crucibles at predetermined temperatures in air.

The furnace temperatures were controlled to within ±1°C. A working thermocouple was positioned next to the sample in the furnace. The working thermocouple was periodically checked against a standard calibrated thermocouple. The overall temperature accuracy was estimated to be ±5°C. Samples equilibrated in air were always quenched in liquid nitrogen to avoid oxidation during cooling. Sample weights were measured before and after the experiments using an analytical balance with an accuracy of ±0.1 mg. The samples were mounted and polished following the final quenching. The sample microstructures were examined in detail using optical as well as Scanning Electron Microscopy (SEM) coupled with energy-dispersive spectra (EDS) analysis. Phase compositions were determined using a JEOL 8800L Electron Probe X-ray Microanalyser (EPMA) with wavelength dispersive detectors. The instrument was operated at 15 kV accelerating voltage with a probe current of 15 nA. $Fe_2O_3$ (Charles M. Taylor, Co., Stanford, CA) and ZnO (prepared in house using ZnO 99.5+ wt pct purity) were used as standards for the EPMA measurements of iron and zinc respectively. The ZnO standard was tested against a certified willemite ($Zn_2SiO_4$) standard (Micro-Analysis Consultants Ltd., Cambridge, United Kingdom). The Duncumb-Philibert ZAF correction procedure supplied with the JEOL-8800L was applied. The average accuracy of the EPMA measurements is within ±1 wt pct.

X-Ray powder Diffraction (XRD) for the purpose of phase identification was carried out with a PHILIPS PW 1130 X-ray diffractometer with a graphite monochromator using Cu K radiation.

### Equilibration and quenching at intermediate $pO_2$s

The $pO_2$ was controlled in the furnace by mixing a high purity 2.07 % $H_2$ in $N_2$ gas mixture with $CO_2$ in proportions calculated for the relevant temperature using FactSage 5.01[6]. The gas-flow was set using mass flow controllers that had been pre-calibrated using a soap-bubble meter to within ±0.5 volume-%. The total gas flow selected varied between 250 and 1000 ml/min. Samples were suspended in a vertical furnace adjacent to the thermocouple in the furnace in an open basket manufactured from Pt. The working tube of the furnace was impermeable recrystallized alumina. Working conditions of the furnace and temperature characteristics of the experiments are comparable to the work performed in air.

To ensure achievement of equilibrium, experiments at $1*10^{-7}$, $1*10^{-6}$ and $1*10^{-4}$ atm $O_2$ in a total pressure of 1 atm were performed by approaching the equilibrium composition from two opposite directions: starting from more oxidized '$Fe_2O_3$'/ZnO ($Fe_2O_3$ and ZnO powder, Fe/(Fe+Zn)=0.35 by moles) and reduced 'FeO'/ZnO (1:1 $Fe_2O_3$:Fe/ZnO powder mixture, Fe/(Fe+Zn)=0.35 by moles) mixtures.

Equilibration of the two samples was achieved according to the following sequence:

- Mixed powder was pelletized and equilibrated at temperature at set conditions.
- The pellet was broken up to pieces ≈1 mm prior to a second equilibration at set conditions.
- The coarse powder was pelletized a second time and equilibrated once more at set conditions.
- Samples were mounted, polished and examined by optical microscopy followed by quantitative EPMA measurements of zincite and spinel.
- Step 2–4 was repeated until compositions of phases in samples approaching equilibria from opposite directions coincided.

Samples produced at intermediate $pO_2$s were quenched in a stream of the reagent gas after lowering into the cool part of the vertical tube furnace.

### Wet-chemical method for the speciation of $Fe^{2+}/Fe^{3+}$

A number of methods for speciation of ferric and ferrous iron were evaluated prior to the development of this methodology. Most procedures require a controlled atmosphere during dissolution of the oxides at high temperatures using different mineral acids; this step can potentially become a source of inaccuracies. A special procedure based on the use of ammonium metavanadate has been developed in the present study. Metavanadate directly oxidizes ferrous iron liberated during the dissolution of zinc-and iron-containing oxides by hydrofluoric acid at room temperature in air. The use of ammonium metavanadate for oxidization of ferrous iron was originally proposed for silicates by Wilson[7] and the further developed procedure is described in detail elsewhere[8]. The main differences between present and the original techniques are the chemicals used for the final titrimetric determination. This methodology is believed to give a more sensitive final titrimetric determination due to the detection of a sharper endpoint.

Ferric iron was calculated as the difference between total and ferrous iron. The method for determination of total iron is described elsewhere[8].

## Results and discussions

### Calculations on the Fe-Zn-O system using FactSage

Degterov *et al.*[9] assessed the studies describing the thermodynamic properties of hematite, spinel, wustite and zincite present in the FeO-$Fe_2O_3$-ZnO system in their paper on the optimization of the Fe-Zn-O system. No information on the ferric and ferrous iron concentrations in zincite is available and there are no experimental studies conducted at intermediate $pO_2$s close to the ZnO-rich corner of the ternary system.

Isothermal sections of the FeO-$Fe_2O_3$-ZnO system at 1000, 1200 and 1450°C were calculated using FactSage[6] and the optimized database[9] and are shown in Figure 1a, 1b and 1c. Several features of the diagrams should be pointed out:

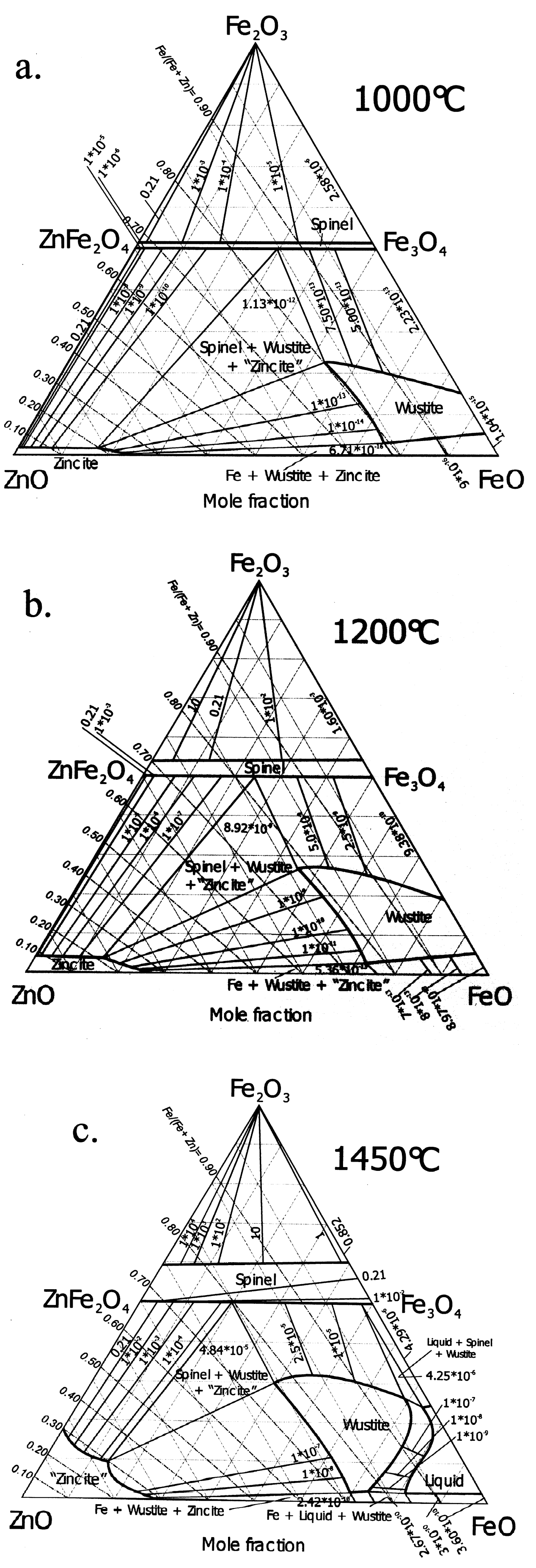

**Figure 1. Predicted isothermal sections of the FeO-$Fe_2O_3$-ZnO system using FactSage[6] and a thermodynamic database[9] at 1000, 1200 and 1450°C in Figures a, b and c respectively**

- The model predicts that the zincite primary phase field extends towards the $Fe_2O_3$ corner with increasing temperature at all $pO_2$s between air and metallic iron saturation.
- The wustite primary phase field expands both in the ZnO and $Fe_2O_3$ direction with increasing temperature.
- The spinel solid solution is becoming more and more non-stoichiometric expanding towards the $Fe_2O_3$-rich side at elevated temperatures. The non-stoichiometry on the ZnO-rich side is very small at these temperatures.
- Equilibrium $pO_2$s are increasing with increasing temperature. The uni-variant equilibrium between spinel, wustite and zincite is predicted to be stable at a $pO_2$ of about $1*10^{-12}$, $1*10^{-10}$ and $1*10^{-5}$ atm at 1000, 1200 and 1450°C respectively.
- The ranges of stability of Fe-Zn-O melts at 1450°C are defined for a range of $pO_2$s.

The predicted diagrams clearly show that zincite and spinel phase can form and coexist under a range of Fe/Zn ratios and oxygen partial pressures.

These initial calculations greatly assist the development of the experimental plan and the evaluation of data.

## The zincite/spinel and spinel/hematite equilibria in air

The compositions of the zincite and spinel phases at equilibrium between 900 and 1580°C in air in the Fe-Zn-O system measured using EPMA are shown in Figure 2 and can be compared to the earlier reported data[9] and predicted phase boundaries calculated using FactSage[6]. The results of the present investigation agree within experimental accuracy with the previously reported experimental data[9]. Figure 3 illustrates the microstructures of the samples of the same bulk composition of Fe/(Fe+Zn) = 0.35 mole at increasing temperatures in air. Both zincite and spinel at equilibrium can be observed in all of the samples (see the dark and light phases respectively). Black spots correspond to pores in the material. The zincite changes from a rounded to a plate-like morphology between 1200 and 1300°C. This transformation of the morphology occurs at the same temperature as the iron concentration in the zincite (visualized in Figure 2) starts to increase significantly.

The ferrous and ferric iron bulk concentrations in samples were determined by wet-chemistry. The spinel is assumed to be stoichiometric $(Fe,Zn)O,Fe_2O_3$ and the Fe/(Fe+Zn) ratios measured with EPMA were used to calculate the concentration of FeO, $Fe_2O_3$ and ZnO respectively in the phase. The FeO/$Fe_2O_3$ concentration in the zincite was subsequently calculated from the mass-balance. This procedure gives small errors in the determination of zincite compositions since negligible deviations from stoichiometry are expected on the ZnO rich side of the spinel solid solution. The zincite composition in two-phase equilibria with spinel from 900 to 1580°C along the air isobar is shown in Figure 4. The FeO mol fraction of the zincite phase gradually increases from insignificant values at 900–1200°C to ~0.06 at 1580°C as temperature increases. The $Fe_2O_3$ mol fraction of the zincite rapidly increases between 1200 and 1300°C from a rather constant level of 0.01 at lower temperatures to nearly 0.17 at 1580°C.

It can be seen from these results that the iron present in zincite in air is in ferric form. This is an unexpected result. First, the stability of $Fe^{2+}$ relative to $Fe^{3+}$ usually increases with increasing temperature as evidenced for, example, by the decomposition of solid $Fe_2O_3$ to $Fe_3O_4$ at 1380°C in air.

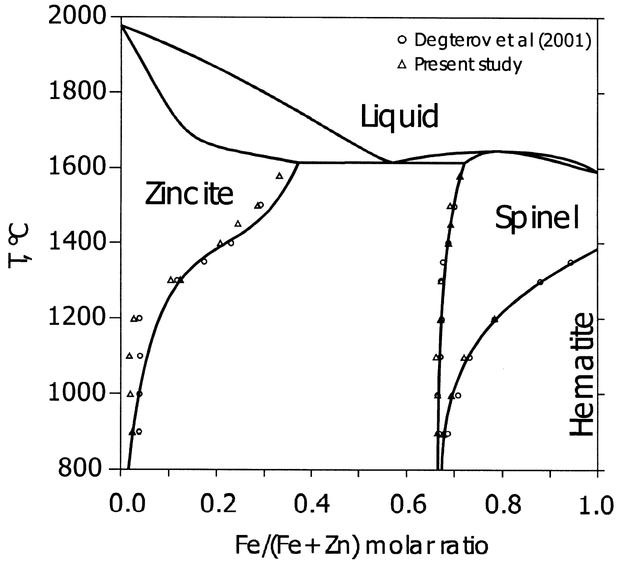

Figure 2. Pseudo-binary phase diagram showing the Fe-Zn-O system in air. Phase boundaries are predicted using FactSage[6] and a thermodynamically optimized database[9]

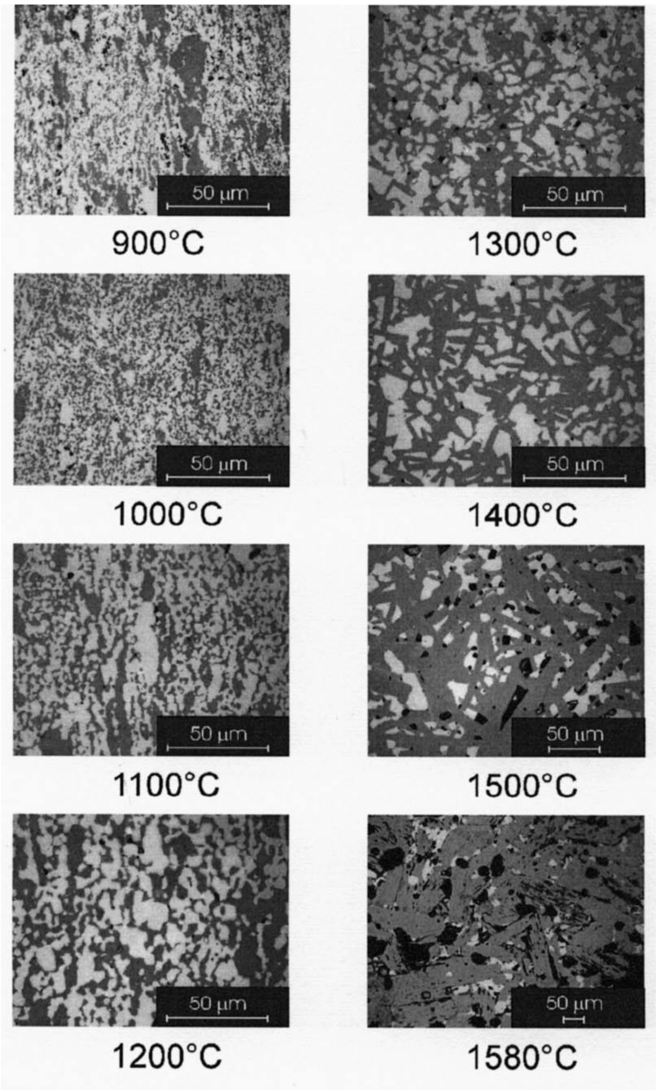

900°C 1300°C

1000°C 1400°C

1100°C 1500°C

1200°C 1580°C

Figure 3. Optical micrographs of samples containing zinc ferrite and zincite in equilibrium in air at 1 atm total pressure starting from a bulk composition of Fe/(Fe+Zn)=0.35 mol. The light, grey and black fields correspond to zinc ferrite, zincite and pores respectively

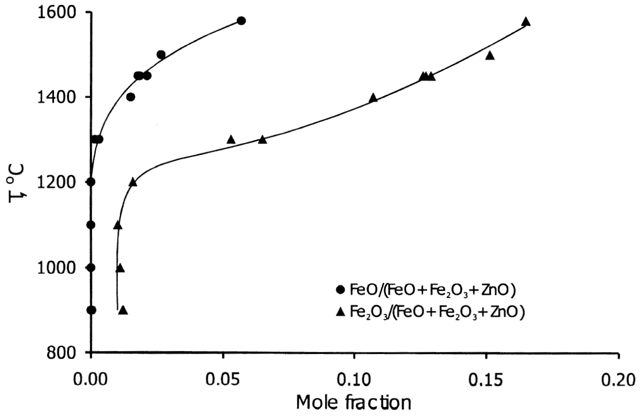

Figure 4. The solubility of ferrous and ferric iron in zincite in equilibrium with spinel in air expressed as mole fractions

In addition, the diameter of both $Zn^{2+}$ and $Fe^{2+}$ (0.60 and 0.63 Å respectively in a 4-fold coordination[10] suggests that the cations easily could change place and thereby form a substitutional solid solution. The ferric iron concentration increases dramatically in zincite in parallel with the change from rounded to plate-like morphology in the same range of temperature. This new information can now be used to investigate the mechanism of the transformation of the zincite morphology and its relation to the $Fe^{2+}/Fe^{3+}$ ratio and $pO_2$. This will enable to better control the shape of zincite.

The hematite and zinc ferrite equilibria were studied between 900 and 1300°C in air. The bulk compositions and compositions of individual phases were determined by wet chemistry and EPMA respectively. The ferrous and ferric iron concentrtion in the spinel phase were re-calculated considering the hematite phase to contain iron oxide only in the ferric form and the ZnO concentration of hematite was measured using EPMA. The inaccuracy introduced by this assumption is negligible since the ferrous iron content of hematite is very low. The present results are compared to those reported by Yamaguchi and Takei[11] in Figure 5. The fraction of FeO in the spinel was found to be higher than previously reported at all temperatures investigated. Present experimental technique is believed to be more accurate since total bulk compositions and the compositions of phases were directly measured using wet chemical analysis and EPMA respectively compared to the previous[11] who estimated the FeO concentrations in the spinel by taking the intersection of the extrapolated extension of measured compositions in the single spinel phase, and extrapolated bulk compositions of FeO in the hematite/spinel two phase equilibria containing different proportions of the phases.

### The zincite and spinel equilibria in intermediate $pO_2$s

The compositions of zincite and spinel in equilibrium at 1200°C and in $pO_2$s equal to $1*10^{-7}$, $1*10^{-6}$ and $1*10^{-4}$ atm and at 1300°C in $pO_2=1*10^{-6}$ atm were determined. The experimentally measured compositions of these phases starting from the '$Fe_2O_3$'-ZnO join and the 'FeO'-ZnO join at each set of conditions of experimental temperatures and $pO_2$ are given in Figures 6 and 7 by circles and crosses respectively. The reproducibility of the measurements at these low $pO_2$s is excellent. The measured composition starting from the '$Fe_2O_3$'-ZnO and the 'FeO'-ZnO join compared to their average is less than ±1 mole-% of FeO, $Fe_2O_3$ and ZnO respectively.

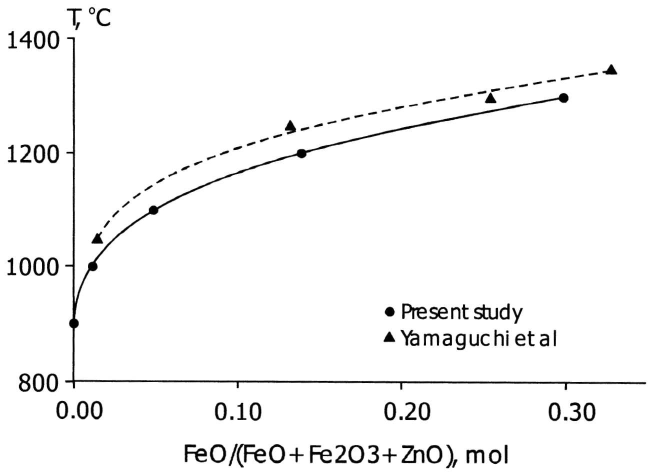

**Figure 5. The ferrous iron concentration in spinel in equilibrium with hematite and air expressed as a function of temperature**

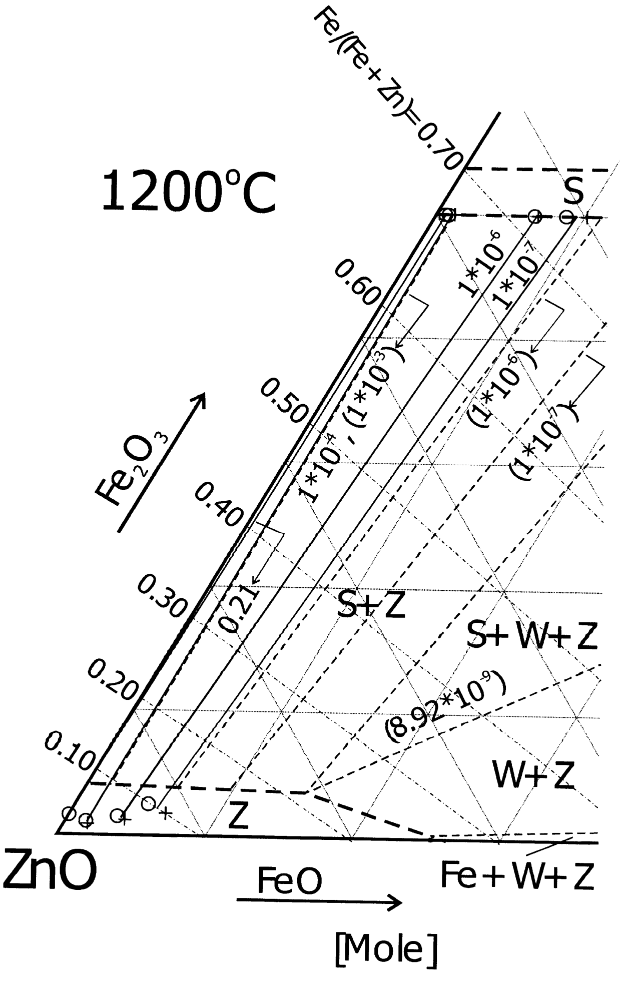

**Figure 6. Enlarged area of the FeO-Fe$_2$O$_3$-ZnO ternary section at 1200°C close to the ZnO-rich corner. Dashed lines are calculated by FactSage[6] and a thermodynamically optimized database[9], and O are used for experimental results from the 'Fe$_2$O$_3$'-ZnO and the FeO-ZnO join respectively in the figure**

At high temperatures and low oxygen partial pressures the vapour pressures of zinc in the gas phase in equilibrium with zincite and spinel can become significant, and zinc is lost to the gas during equilibration of the samples. In the present experiments the achievement of local equilibrium in the condensed phases has been carried out through equilibration of different starting materials—the test being that the compositions of the individual phases are uniform throughout the samples, and identical to those in samples prepared from different starting materials but at different temperatures and oxygen partial pressures.

It is evident from Figure 6 that the concentration of FeO in zincite in equilibrium with spinel is higher at more reducing conditions, and it appears that the Fe$_2$O$_3$ concentration is slightly increased. This is expected since Fe$^{2+}$ generally is becoming more stable in relation to Fe$^{3+}$ at decreasing pO$_2$s. It also agrees with the discussion on cation size in the previous section. The concentration of FeO in the spinel in equilibrium with zincite is also increasing at decreasing pO$_2$s at the expense of ZnO decreasing at equal levels assuming the spinel to be stoichiometric.

The zincite primary phase field expansion in both the FeO and Fe$_2$O$_3$ direction from 1200 to 1300°C in pO$_2$=1*10$^{-6}$ atm is shown in Figure 7. Both the trends of increasing ferric and ferrous iron concentrations in the zincite observed at increasing temperatures in air and decreasing pO$_2$s (at 1200°C) respectively are confirmed. The concentration of FeO in the spinel, equilibrated with zincite, is increasing with increasing temperature.

A comparison between the experimental results and predictions by FactSage[6] are shown in Figures 6 and 7. Predicted phase boundaries and tie lines at specific oxygen

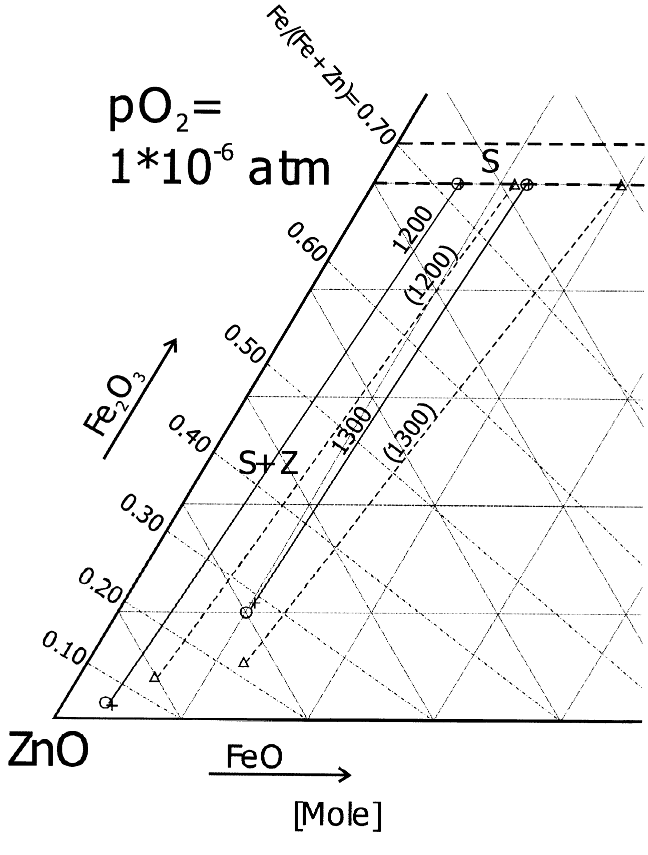

**Figure 7. Enlarged area of the FeO-Fe$_2$O$_3$-ZnO ternary diagram at pO$_2$=1*10$^{-6}$ atm close to the ZnO-rich corner. Dashed lines are calculated by FactSage[6] and a thermodynamically optimized database[9], and O is used for experimental results from the 'Fe$_2$O$_3$'-ZnO and the FeO-ZnO join respectively, and Δ is used for predicted compositions**

partial pressures are given as dashed lines in the figures. The general trend of increasing ferrous iron concentrations in the zincite at more reducing conditions shown in Figure 6 is well described by the optimized thermodynamic model. The differences between determined and calculated ferrous iron concentrations in both the spinel and zincite solid solutions increase with decreasing $pO_2$s. The effective oxygen partial pressures of predicted tie lines are about one order of magnitude lower than the measured ones. Considering no data was available for these conditions at the time the optimization of the thermodynamic model was undertaken this appears to be a reasonable estimate. Figure 7 shows that both the ferrous and ferric iron concentration in the zincite phase in equilibrium with spinel is somewhat overestimated by the model at 1200°C while being underestimated at 1300°C in $pO_2=1*10^{-6}$ atm. The concentrations of ferrous iron in zinc ferrite solid solution are being overestimated by the model at both temperatures and $pO_2=1*10^{-6}$ atm.

## Implications to industrial practice

In industrial practise the formation of plate-like zincite was first observed in zinc blast furnace sinters; these chemically complex materials consists principally of zincite, spinel and liquid slag phases. The present study has shown that the plate-like zincite morphology can also be formed in the absence of the slag phase, and that its appearance is dependent on the temperature, iron/zinc ratio in the zincite and the oxygen partial pressure of the system. The implications of these findings are that the conditions for change in zincite morphology are related to the thermodynamic properties of the system rather than the mechanism of formation.

The new experimental data on the phase equilibria in the Fe-Zn-O system described in the present study provides the link between solid, and liquid phase equilibria—information essential for the improvement of the existing thermodynamic models of the zinc smelting slag systems.

It will then be possible to accurately predict, for example, the formation of zincite and spinel phases in ISP sinters at high oxygen partial pressure, and the formation of wustite, zincite and spinel in ISP slags, the liquidus temperatures and proportions of solids and liquid phases present in these systems.

## Conclusions

Experimental work has been undertaken on the Fe-Zn-O system in air and at intermediate $pO_2$s. The ferric and ferrous iron concentrations in zincite in equilibrium with spinel have been determined between 900 and 1580°C in air using a specially developed wet-chemical procedure. Predictions by FactSage that iron dissolved in zincite is predominately in the ferric form were confirmed. The increasing concentration of ferric iron in zincite coincides with a change of morphology of the phase from rounded to plate-like between 1200 and 1300°C.

Tie lines showing the composition of both zincite and spinel at intermediate $pO_2$s equal to $1*10^{-7}$,$1*10^{-6}$, $1*10^{-4}$ and 0.21 atm has been determined at 1200°C and at 1300°C for the $1*10^{-6}$ atm $pO_2$ isobar.

The current version of the thermodynamically optimized database has been used in conjunction with the FactSage program to describe phase equilibria in the Fe-Zn-O system and these predictions have been compared with the new experimental data.

## Acknowledgement

The authors thank the Australian Research Council for ongoing support for this research. We also would like to thank the ISP Smelting Companies Britannia Zinc Ltd, Portovesme SRC, MIM Huttenwerke Duisburg GmbH, Hachinohe Smelting Company Ltd and Pasminco Smelter Technical Support for financial support of this project.

## Refernces

1. HOLLIDAY, R.J. and SHOOBRIDGE, P.H. A Study of the Composition, Microstructure and Softening Characteristics of some Zinc-Lead Sinters. Aus. *I.M.M. Conference*. North Queensland. 1978, pp. 311–321.
2. HOLLIDAY, R.J., SHOOBRIDGE, P.H., and FIRKIN, G.R. The Influence of Microstructure and Softening Cheracteristics of Zinc-Lead Sinter on the Operation of an Imperial Smelting Furnace. *Aus. Jap. Extr. Metall. Symp*. Sydney, Australia. 1980, pp. 343–351.
3. LEE, F.T. and HAYES, P.C. Microstructural Changes on the Reduction of Imperial Smelting Furnace Sinters. *Metall. Mater. Trans. B*, vol. 24B, no. 1. 1993. pp. 39–51.
4. ZHAO, B., JAK, E., and HAYES, P.C. Initial Softening Behaviour of ISP Sinter. *Metallurgical High Technology and new Materials of Heavy Nonferrous Metals*. Kunming, China. Yunnan Science and Technology Press. 2002, pp. 593–600.
5. JAK, E., HAYES, P.C., and LEE, H.G. Improved Methodologies for the Determination of High Temperature Phase Equilibria. *Kor. IMM J.*, vol. 1, no. 1. 1995. pp. 1–8.
6. BALE, C.W., *et al.* FactSage Thermochemical Software and Databases. *CALPHAD*, vol. 26, no. 2. 2002. pp. 189–228.
7. WILSON, A.D. The Micro-determination of Ferrous Iron in Silicate Minerals by a Volumetric and Colorimetric Method. *Analyst*, vol. 85, 1950. pp. 823–827.
8. HANSSON, R., HAYES, P.C., and JAK, E. Phase Equilibria in the Fe-Zn-O System in Air with Special Attention to the ZnO-Rich Area. Manuscript, 2002.
9. DEGTEROV, S.A., *et al.* Experimental Study of Phase Equilibria and Thermodynamic Optimization of the Fe-Zn-O System. *Metall. Mater. Trans. B*, vol. 32, 2001. pp. 643–657.
10. SHANNON, R. Revised Effective Ionic Radii and Systematic Studies of Interatomic Distances in Halides and Chalcogenides. *Acta Crystallographica*, vol. A32, 1976. pp. 751–767.
11. YAMAGUCHI, T. and TAKEI, T. Phase Diagram and Dissociation Characteristics in the Ferrite Region of the System Zn-Fe-O in Oxygen Pressure of the Atmosphere. *Sci. Pap. Inst. Physic. Chem. Res.*, vol. 53, no. 1517. 1959. pp. 207–215.